11 Radial Equilibrium

In Chapter 5 we briefly described a simple radial equilibrium condition necessary to determine the radial distribution of the stage parameters such as, ϕ, λ, r, α_i, and β_i. Assuming an axisymmetric flow with constant meridional velocity and total pressure distributions, we arrived at free vortex flow as a simple radial equilibrium condition with $rv_u = const.$ In practice, from aerodynamics design point of view a constant meridional velocity component or constant total pressure may not be desirable. As an example, consider the flow field close to the hub or tip of a stage, where secondary flow vortices predominate. As discussed in Chapter 6, these secondary vortices induce drag forces leading to secondary flow losses which reduce the efficiency of the stage. To reduce the secondary flow losses, specific measures can be taken that are not compatible with the simple radial equilibrium condition. In this case the simple radial equilibrium method needs to be replaced by a general one. Wu [1] proposed a general theory for calculating the three-dimensional flow in turbomachines. He introduced two sets of surfaces: Blade to blade surfaces called S_{1i} and hub-to-tip surfaces labeled with $S_{2j.}$ Utilizing S_{1i} and S_{2j} surfaces, Wu [1] proposed an iterative method to solve the three-dimensional inviscid flow field in turbomachinery stages. Coupling both surfaces, however, is associated with computational instabilities that gives rise to replacing the technique by complete Euler or Navier-Stokes solver, [2]. A computationally more stable method for solving the flow field is the streamline curvature technique. This method is widely used in turbomachinery industry and is the essential tool for generating the basic design structure necessary to start with CFD application. Streamline curvature method can be used for design, off-design, and analysis. Vavra [3] presented the theoretical structure for inviscid axisymmetric flow in turbomachines that can be used to derive the streamline curvature equations. A thorough review of the streamline curvature method can be found in Novak and Hearsey [4], Wilkinson [5], and Lakshminarayana [2].Wennerstrom [6] presented a concise description of this technique, which is given in this section in its original form.

Rapid calculation procedures used in the turbomachinery industry determining the distribution of flow properties within the turbomachinery assume steady adiabatic flow and axial symmetry. The more sophisticated of these procedures include calculation stations within blade rows as well as the more easily treated stations at the blading leading and trailing edges. The assumption of axial symmetry in the bladed region implies an infinite number of blades. The blade forces acting between the

blades and the fluid are taken into consideration by body force terms in equation of motion. The streamlines are not straight lines as could be supposed. They usually have certain curvatures that are maintained if the forces exerted on the fluid particle are in equilibrium state, described by the equilibrium equation. This equation includes various derivatives in the meridional plane and is solved in this plane along the computing stations which are normal to the average meridional flow direction. The equilibrium equation in its complete form cannot be solved analytically, therefore numerical calculation methods are necessary. For the application of the equilibrium equation to the stage flow with streamline curvature, Hearsey [7] developed a comprehensive computer program, which is successfully used in the turbomachinery industry for design of advanced compressors and turbines. Since the treatment of the corresponding numerical method for the solution of this equation is given in [7], this chapter discusses the basic physical description of the calculation method. As a result, streamline curvature method can be used as design tool and for the post design analysis. An advanced compressor design is presented followed by a brief discussion of special cases.

11.1 Derivation of Equilibrium Equation

The starting point for this derivation is the formulation of the equations of motion for an axisymmetric flow in intrinsic coordinates fixed in space along streamlines as shown in Fig.11.1.

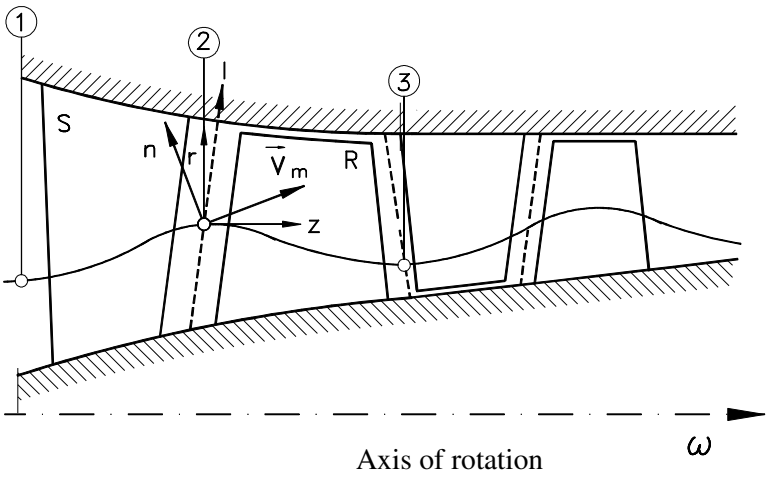

Fig. 11.1: Flow through axial compressor, streamline, directions are: n = normal, m = meridional, r = radial, z = axial, and l = computing station

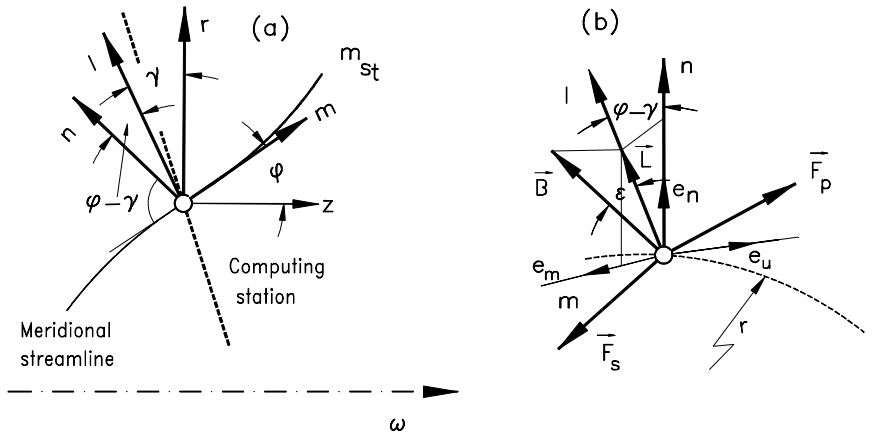

Fig. 11.2: (a) Coordinate directions in the meridional plane, (b) orientation of vectors with respect to m, u, n orthogonal coordinate system, redrawn from [6].

The momentum equation in meridional direction:

$$V_m \frac{\partial V_m}{\partial m} - \frac{V_u^2}{r} \sin\phi = -\frac{1}{\rho}\frac{\partial p}{\partial m} + F_m \tag{11.1}$$

in stream surface normal direction:

$$\frac{V_m^2}{r_c} - \frac{V_u^2}{r} \cos\phi = -\frac{1}{\rho}\frac{\partial p}{\partial n} + F_n \tag{11.2}$$

and in circumferential direction:

$$\frac{V_m}{r}\frac{\partial (rVu)}{\partial m} = F_u \tag{11.3}$$

Thermodynamic equations required are the energy equation for steady adiabatic flow:

$$H = h + \frac{V^2}{2} \tag{11.4}$$

and the Clausius-Gibbs relation:

$$\frac{1}{\rho} dp = dh - Tds \tag{11.5}$$

Since, in intrinsic coordinates, there is no velocity component in the n-direction (by definition),

$$V^2 = V_m^2 + V_u^2 \tag{11.6}$$

Equations (11.4), (11.5), and (11.6) are combined to give:

$$\frac{1}{\rho} dp = dH - Tds - V_m dV_m - V_u dV_u \tag{11.7}$$

Since the computation station lies in the space between the stator and the rotor usually not normal to the meridional stream surface, the derivatives must be defined with respect to the l-direction along a computing station, Fig.11.2:

$$\frac{d}{dl} = \frac{dn}{dl}\frac{\partial}{\partial n} + \frac{dm}{dl}\frac{\partial}{\partial m} = \cos(\phi - \gamma)\frac{\partial}{\partial n} + \sin(\phi - \gamma)\frac{\partial}{\partial m} \tag{11.8}$$

Rearranging Eq.(11.8) to eliminate the derivatives with respect to the normal direction:

$$\frac{\partial}{\partial n} = \sec(\phi - \gamma)\frac{d}{dl} - tg(\phi - \gamma)\frac{\partial}{\partial m} \tag{11.9}$$

Introducing Eq.(11.7) into Eq.(11.1) and (11.2), eliminating derivatives with respect to *n* with Eq.(11.9), the resulting equations are combined to eliminate

$$\frac{\partial H}{\partial m} - T\frac{\partial s}{\partial m} \tag{11.10}$$

The equation obtained after algebraic rearrangement and trigonometric substitution is:

$$V_m \frac{dV_m}{dl} = \sin(\phi - \gamma) V_m \frac{\partial V_m}{\partial m} + \cos(\phi - \gamma)\frac{V_m^2}{r_c} - \frac{V_u}{r}\frac{d(rV_u)}{dl} +$$

$$\frac{dH}{dl} - T\frac{ds}{dl} - \sin(\phi - \gamma)F_m - \cos(\phi - \gamma)F_n \tag{11.11}$$

In some cases, it is more convenient to work in a similar system of coordinates which is stationary with respect to a rotating blade row. As shown in Chapter 3, Eq.(11.11) is easily transformed into the rotating frame of reference by introducing the substitution:

$$V_u = W_u + \omega r \tag{11.12}$$

for the circumferential velocity component. The corresponding relative total enthalpy[1] H_r from Eq. (3.104) is:

$$H_r = h + \frac{W^2}{2} - \frac{U^2}{2} \tag{11.13}$$

Combining Eqs. (11.12), and (11.13) leads to:

$$H = H_r + \omega r\left(W_u + \omega r\right) \tag{11.14}$$

Introducing Eqs.(11.12) and (11.14) into Eq. (11.11), the corresponding radial equilibrium equation is:

$$V_m \frac{dV_m}{dl} = \sin(\phi - \gamma)\, V_m \frac{\partial V_m}{\partial m} + \cos(\phi - \gamma)\, \frac{V_m^2}{r_c} - \frac{W_u}{r} \frac{d(rW_u)}{dl} +$$

$$\frac{dH_r}{dl} - T\frac{ds}{dl} - 2\omega W_u \cos\gamma - \sin(\phi - \gamma)\, F_m - \cos(\phi - \gamma)\, F_n \tag{11.15}$$

Equations.(11.11) and (11.15) represent the radial equilibrium condition. The point of principal interest in this derivation are associated with the treatment of the body forces, F_m and F_n. Note that the complete body force field contains a third component F_u which is orthogonal to the other two mutually orthogonal components F_m and F_n and can be directly calculated from Eq. (11.3). The reminder of this derivation is aimed at obtaining expressions for F_m and F_n which relate to geometric properties of the blading. Combining Eqs.(11.1) and (11.7) gives:

$$T\frac{\partial s}{\partial m} = \frac{\partial H}{\partial m} - \frac{V_u^2}{r}\sin\phi - V_u \frac{\partial V_u}{\partial m} - F_m \tag{11.16}$$

---

[1] Wennerstrom [6] calls this quantity rothalpy which was introduced by Wu [1], who termed the sum of the static enthalpy and the kinetic energy of the relative flow $h_R = h + W^2/2$ as the relative total enthalpy (see also Lakshminarayana [2]). In a rotating frame of reference, the expression h_R changes along a streamline that varies in radial direction. In contrast, the relative total enthalpy given by Eq. (11.13) derived in Chapter 3 (Eq. 3.104) remains constant and is generally valid within a rotating frame of reference, where the streamlines may change in radial direction (see also Vavra [3]).

or

$$T\frac{\partial s}{\partial m} = \frac{\partial H}{\partial m} - \frac{V_u}{r}\frac{\partial (rV_u)}{\partial m} - F_m \tag{11.17}$$

Equation (11.3) and the thermodynamic definition of work (applied to a turbomachine) may be combined to give

$$\frac{\partial H}{\partial m} = \frac{U}{r}\frac{\partial (rV_u)}{\partial m} \tag{11.18}$$

a differential form of the Euler equation of turbomachinery. Combining Equations (11.17) and (11.18), noting from the velocity triangle that

$$tg\beta = \frac{W_u}{V_m} \tag{11.19}$$

and introducing Equation (11.3) again leads to

$$F_m = -F_u \tan\beta - T\frac{\partial s}{\partial m} \tag{11.20}$$

Equation (11.20) is sufficient to solve Eqs. (11.11) or (11.15) for some bladeless cases but, in order to solve the equations within a bladed region, more information is required concerning the direction and nature of the force components. For this purpose, it is convenient to resort to vector analysis to relate the various force components and coordinate directions. Fig.11.2b illustrates the vectors described in the following discussion. The variables *m, u, n* are the principal orthogonal axes of a right handed, streamline coordinate system. In this system, F_s is the body force vector acting to oppose motion of the fluid; i.e. the body force which produces an irreversible increase in entropy. It lies in the m-u plane and at the angle β (relative flow angle) from the meridional direction. The vector $\boldsymbol{L}$ is coincident with the l-direction and lies in the n-m plane at the angle (ϕ-γ) from the n-direction. The vector B is tangent to the mean blade surface and lies in the l-u plane at an angle ε from the l-direction. Planes such as the m-u plane and l-u plane are understood as planes tangent to the curved surface described by the respective coordinates at the point in question. The equation of the unit vector in F_s-direction is:

$$\frac{\boldsymbol{F_s}}{F_s} = \cos\beta\, e_m + \sin\beta\, e_u + (0)\, e_n \tag{11.21}$$

and the equation of the unit vector $\boldsymbol{B}$ is

$$\boldsymbol{B} = \cos\varepsilon\sin(\phi - \gamma)e_m - \sin\varepsilon\, e_u + \cos\varepsilon\cos(\phi - \gamma)e_n \tag{11.22}$$

The force due to a pressure difference across a blade acts in a direction normal to both vectors $\boldsymbol{F}_s$ and $\boldsymbol{B}$, which together define the local plane of the mean blade surface at a point. Therefore, pressure force vector can be defined by the cross product of $\boldsymbol{F}_s$ and $\boldsymbol{B}$. Since $\boldsymbol{F}_s$ and $\boldsymbol{B}$ are usually not perpendicular but at an angle $(\pi/2 - (\phi - \gamma))$ to one another, the product of these vectors differs from a unit vector by $\cos(\phi - \gamma)$. Therefore to obtain a unit vector for the force due to pressure across a blade and because $\boldsymbol{F}_p$ must be positive direction of rotation, this is written

$$\frac{\boldsymbol{F}_p}{F_p} = \frac{1}{\cos(\phi - \gamma)}\left[\frac{\boldsymbol{B}\times\boldsymbol{F}}{F_s}\right]$$

$$\frac{\boldsymbol{F}_p}{\boldsymbol{F}_p} = -\sin\beta\cos\varepsilon\, e_m + \cos\beta\cos\varepsilon\, e_u + \left[\frac{\cos\beta\sin\varepsilon}{\cos(\phi-\gamma)} + \sin\beta\cos\varepsilon\, tg(\phi - \gamma)\right] \tag{11.23}$$

From Fig.11.2b, note that $\boldsymbol{F}_m$ is composed of the m-components of $\boldsymbol{F}_s$ and $\boldsymbol{F}_p$. Consequently, from Eqs.(11.21) and (11.23):

$$F_m = F_s\cos\beta - F_p\sin\beta\cos\varepsilon \tag{11.24}$$

Similarly, $\boldsymbol{F}_u$ and $\boldsymbol{F}_n$ are composed respectively of the u and n components of $\boldsymbol{F}_s$ and $\boldsymbol{F}_p$

$$F_u = F_s\sin\beta + F_p\cos\beta\cos\varepsilon \tag{11.25}$$

$$F_n = F_p\left[\cos\beta\sin\varepsilon\sec(\phi - \gamma) + \sin\beta\cos\varepsilon\, tg(\phi - \gamma)\right] \tag{11.26}$$

Since the orthogonal components of the force field have been defined in terms of components acting along and perpendicular to the relative flow direction, it is possible to solve for these two components. By inserting Eqs.(11.24) and (11.25) into Eq. (11.20) and simplifying, one obtains:

$$F_s = -\cos\beta\, T\frac{\partial s}{\partial m} \tag{11.27}$$

Subsequently, Eqs.(11.25) and (11.27) can be combined to give

$$F_p = \frac{F_u}{\cos\beta\cos\varepsilon} + \frac{\sin\beta}{\cos\varepsilon} T\frac{\partial s}{\partial m} \tag{11.28}$$

If Eqs.(11.27) and (11.28) are now inserted into Eqs.(11.24) and (11.26) , the body forces appropriate to the intrinsic coordinate system are defined in terms of parameters readily calculated. The most useful form of the radial equilibrium equation is the form in relative system, Equation (11.15), since it becomes identical to Eq.(11.11) in the absolute system when the angular velocity of the coordinates is set equal to zero. Combining Eq.(11.24), (11.26), (11.27) and (11.28) into Eq.(11.15) puts the radial equilibrium equation in the form:

$$V_m \frac{dV_m}{dl} = \sin(\phi - \gamma) V_m \frac{\partial V_m}{\partial m} + \cos(\phi - \gamma) \frac{V_m^2}{r_c} -$$

$$\frac{W_u}{r} \frac{d\left(r W_u\right)}{dl} + \frac{dH_r}{dl} - T\frac{ds}{dl} - 2\omega W_u \cos\gamma - tg\varepsilon F_u +$$

$$\left[\sin(\phi - \gamma)\cos^2\beta - tg\varepsilon \sin\beta \cos\beta\right] T\frac{\partial s}{\partial m} \tag{11.29}$$

The force $\boldsymbol{F_u}$ can be obtained from Eq.(11.3) or from

$$F_u = \frac{V_m}{r} \frac{\partial (r W_u)}{\partial m} + 2\omega V_m \sin\phi \tag{11.30}$$

applicable to the relative system. If working in a relative system with specified flow angle, it is convenient to employ Eq.(11.19) to eliminate W_u. The result of this substitution included in a combined form of Eq.(11.29) and (11.30) is

$$V_m \frac{dV_m}{dl} = \cos^2\beta \left[\left(\sin(\phi - \gamma) - tg\varepsilon\, tg\beta\right) V_m \frac{\partial V_m}{\partial m} + \cos(\phi - \gamma) \frac{V_m^2}{r_c} \right] -$$

$$\cos^2\beta \left[V_m^2 \frac{tg\beta}{r} \frac{d(rtg\beta)}{dl} - 2\omega V_m \left(tg\varepsilon \sin\phi + tg\beta \cos\gamma\right) \right] +$$

$$\cos^2\beta \left[\left(\sin(\phi - \gamma)\cos^2\beta - tg\varepsilon \sin\beta \cos\beta \right) T\frac{\partial s}{\partial m} \right] +$$

$$\cos^2\beta \left[\frac{dH_r}{dl} - T\frac{ds}{dl} - V_m^2 \frac{tg\varepsilon}{r} \frac{\partial (rtg\beta)}{\partial m} \right] \tag{11.31}$$

The form of the radial equilibrium equation most appropriate for a particular calculation depends on a number of factors. The most important of these are the nature of the numerical scheme for analysis and the choice of parameters to be specified. This derivation was guided by the intent to apply the results to a streamline curvature type of computing procedure wherein the meridional velocity was the primary variable for which solutions were sought. In this type of procedure, the radial equilibrium equation is solved along each computing station for an assumed set of streamlines. The streamlines are then refined and this process repeated until a satisfactory degree of convergence is attained. This calculation method is used successfully in turbomachinery industry for design of advanced compressors and turbines.

Before discussing applications in bladed regions of a turbomachine, consider applications involving bladefree spaces. The body force due to a pressure difference across a blade was defined by the vector F_p in Eq.(11.23). In a bladefree space, this component is zero. The remaining body force, F_s, associated with the entropy increase was defined by Eq.(11.26). Hence, Eqs.(11.24), (11.25) and (11.26) describing the three orthogonal body forces of the intrinsic coordinate system reduce to

$$F_m = -\cos^2\beta\, T\frac{\partial s}{\partial m} \tag{11.32}$$

$$F_u = -\sin\beta\cos\beta T\frac{\partial s}{\partial m} \tag{11.33}$$

$$F_n = 0 \tag{11.34}$$

In addition, all terms involving the blade lean angle, ε, drop out of the radial equilibrium equation. Equation (11.29) then reduces to:

$$V_m\frac{dV_m}{dl} = \sin(\phi-\gamma)V_m\frac{\partial V_m}{\partial m} + \cos(\phi-\gamma)\frac{V_m^2}{r_c} -$$

$$-\frac{W_u}{r}\frac{d(rW_u)}{dl} + \frac{dH_r}{dl} - T\frac{ds}{dl} - 2\omega W_u\cos\gamma +$$

$$+\sin(\phi-\gamma)\cos^2\beta\, T\frac{\partial s}{\partial m} \tag{11.35}$$

It is interesting to note that according to Eq.(11.32) and (11.33) in a swirling flow, an entropy rise in the direction of flow always leads to body force terms both in — and

u-directions. This is obvious for the vaneless diffuser and a centrifugal machine where most of the entropy rise occurs from wall friction. It is much less obvious for an axial turbomachine of high aspect ratio where annulus wall friction may be negligibly small in relation to losses due to wake mixing. However, it appears that a change in angular momentum occurs in both cases if the entropy is assumed to be increasing in flow direction.

Considering bladed regions, the choice of parameters specified initially generally falls into one of two categories. The first involves cases where total temperature or circumferential velocity component is specified. Practically these variables are for all practical purposes interchangeable, being simply related through Eq.(11.18). The most convenient solution for these cases is usually obtained in stationary frame of reference using Eq.(11.29) with $\omega = 0$, $W_u = V_u$, and $H_r = H$. During each calculation pass, the only variables in Eq.(11.29) are usually V_m and β, since all the other parameters distributed along the *l*-direction are either input data or upgraded between passes. The second important category of calculation within the bladed region involves specified relative flow angles. For this purpose it is most expedient to work in a relative frame of reference, specifying ω within the rotors and zero elsewhere. The most convenient radial equilibrium equation is Eq.(11.31). In this instance, the only variable in Eq.(11.31) during a calculation pass is V_m and all other variations in *l*-direction are either input data or upgraded only between calculation passes.

11.2 Application of Streamline Curvature Method to Turbomachinery

Utilizing the equations derived in section 11.1, Hearsey [7] developed a computational tool that can be used for design and analysis of turbomachines. This section summarizes the computational aspects of the streamline curvature technique by Hearsey [7].

As discussed in the previous section, the streamline curvature method offers a flexible method of determining an Euler solution of the axisymmetric flow through a turbomachine. The computational grid comprises the streamlines, as seen in a meridional view of the flow path, and quasi-normals that are strategically located in the flow, Figs. 11.1. Several stations are generally placed in the inlet duct upstream of the turbomachine proper, and several more are generally placed downstream. Within the turbomachine, the minimum number of quasi-normals, or "stations", is simply one between each adjacent pair of blade-rows, which would then represent both outlet conditions from the previous row and inlet conditions to the next. A better choice is one at each edge of each blade-row. For some calculations, additional stations are added within the blade-rows. This is a relatively coarse grid (compared with that used for CFD computations), making for calculations that typically take just seconds to complete (when run on a typical year-2003 PC).

By virtue of being an axisymmetric, Euler solution, the basic method is inherently incapable of predicting entropy rises, that is pressure losses and efficiency. This is handled by invoking a cascade performance prediction scheme to estimate losses and, in some situations, discharge flow angles from blading. Complicated boundary layers form on the flow path inner and outer walls of turbomachinery, causing "blockage" and participating in secondary flows. Especially for multi-stage axial compressors, a good estimate of blockage is required in order to correctly predict stage matching.

The equation system that is used broadly caters to two situations: when the variation of absolute tangential velocity component along a computing station is known, and when the relative flow angle distribution is known. The former generally arises in "design" calculations, and the latter in "analysis", or performance prediction, cases. Thus the streamline curvature procedure may be used for design calculations, off-design performance predictions and test-data analysis. This versatility, combined with the speed of solution, makes the method a work-horse tool. Many designs can be accomplished using only the streamline curvature method, and while some CFD computations are now offering design capability, even then a good candidate design is generally required as a starting point.

Although the Euler equations are the basis of the method, properly accounting for the change in entropy that is super-imposed from station to station, that is, in the streamwise direction, requires some care. This was highlighted in Horlock [8] in which several previously-published equation systems were examined and found to be missing what is usually a small term.

For the case where tangential velocities are known, the appropriate equation is Eq. (11.29). When relative flow angles are known, Eq. (11.31) is used. In conjunction with one of these equations, the continuity equation and the energy equation are required. Fluid properties are also required; these are best computed in a discreet sub-program to allow for easy replacement. The continuity equation takes the form:

$$\dot{m} = \int_{r_h}^{r_t} V_m \rho \cos(\phi - \gamma) 2\pi r dl \tag{11.36}$$

The rate of change of flow with meridional velocity will also be required. This is given by:

$$\frac{d\dot{m}}{dV_m} = \int_{r_h}^{r_t} (1 - M_m^2) \frac{d\dot{m}}{V_m} \tag{11.37}$$

when tangential velocity component is specified, or:

$$\frac{d\dot{m}}{dV_m} = \int_{r_h}^{r_t} \left[1 - M_{m_{rel}}^2 \left(1 + \frac{\zeta \kappa p/P_{rel}}{1 + \zeta(1 - p/P_{rel})} \right) \right] \frac{d\dot{m}}{V_m} \tag{11.38}$$

when relative flow angle is given. The loss coefficient ζ included in Eq. (11.38) is the total pressure loss coefficient normalized by *exit* dynamic pressure. If not used, it is set zero in Eq. (11.38). The Euler equation of turbomachinery relates total enthalpy change to angular momentum change:

$$\Delta H = H_3 - H_2 = \omega(r_3 V_{u3} - r_2 V_{u2}) \tag{11.39}$$

11.2.1 Step-by-Step Solution Procedure

Given these equations, a step-by-step procedure to obtain a solution is as follows:

(1) An initial estimate of the streamline pattern is made. An obvious choice is to divide the flow path into equal areas at each station. Slightly more uniform (final) streamline spacing may be achieved by dividing the inlet (or some other) station into equal increments, and then using the resulting area fractions to guide the remaining estimates.

(2) Initial estimates of the streamwise gradients that occur in Eqs.(11.29) and (11.31) are made. These are all second-order terms, and zero is the usual first estimate.

(3) The streamline slopes and curvatures are computed at all mesh points (although alternatively this can be done station-by-station as the calculation proceeds). Curvatures are normally set to zero for the first and last stations.

(4) At the first station, the user is required to specify the variation of total enthalpy, entropy and angular momentum or flow angle along the station. Enthalpy and entropy are typically implied by total pressure and temperature in the users input data. The fluids package can then be used to obtain enthalpy and entropy on each streamline.

(5) A first estimate of the meridional velocity on one streamline is made, from the inlet flow and the first station area. It is recommended that the mid-streamline value be defined. High accuracy is not required. (This will not be required after the first pass).

(6) Depending upon whether angular momentum or flow angle was given in the input data, Eq. (11.29)or (11.31) is integrated from the mid-streamline to the inner wall, and from the mid-streamline to the outer wall. This yields a meridional velocity distribution that is consistent with the momentum equation, the assumed streamline characteristics and the estimated mid-line velocity estimate. Although this is not likely to occur at Station 1, extreme values can lead to negative velocities, or values greater than the speed of sound. Provisions must be made for such occurrence.

(7) Equations (11.36) and (11.37) or (11.38) are integrated across all streamlines, to yield the achieved flow and its rate of change with meridional velocity.

(8) The sign of the flow gradient indicates on which branch of the continuity equation the current velocity profile lies, a positive value indicating the subsonic branch and a negative value the supersonic branch. If tangential velocity is specified, only the subsonic branch is valid for a streamline curvature solution but if flow angle is specified, the user must specify which branch is required; both are potentially valid. (The criterion for a valid solution is actually that the meridional velocities be less than the speed of sound. Thus if zero or small flow angles are specified, the supersonic solution will not be valid). If the profile lies on the correct branch, and the achieved flow is within the desired tolerance of the specified flow, control passes to Step 9. Otherwise a new estimate of the mid-line meridional velocity is required. If the profile lies on the wrong branch, a semi-arbitrary change in the mid-line meridional velocity estimate is made, and control returns to Step 6 (subject to some limit on the permitted number of iterations). Otherwise, the mid-line meridional velocity is re-estimated using:

$$V_{m_{new}} = V_{m_{old}} + \frac{\left(\dot{m}_{specified} - \dot{m}_{achieved}\right)}{\frac{d\dot{m}}{dV_m}} \tag{11.40}$$

and again, control returns to Step 6 (subject to some limit on the permitted number of iterations). Several potential difficulties exist when applying Eq. (11.40). The gradient $d\dot{m}/dV_m$ becomes ever smaller as the junction between the two branches of the continuity equation is approached. Thus very large changes in *Vm*-mid may be calculated (although usually not at Station 1, but this same procedure will be used at stations). Some logic should therefore be employed to ensure that the result of applying Eq. (11.39) is plausible.

(9) The process moves on to the next station. Although Station 2 will usually be in an inlet duct, a general description applicable to all stations after the first will be given.

(10) If the station follows a blade-free space, total enthalpy, entropy and angular momentum are convected along streamlines from the previous station (these

may have to be computed following a solution at the previous station if Eq. (11.29) or (11.31) in rotating coordinates was used). Equation (11.29) will be applied whenever absolute angular momentum is given or implied by the user input data. Equation (11.39) will usually be used to determine total enthalpy from angular momentum, or vice versa. Entropy is determined from the efficiency or pressure loss, however expressed. In some cases, for example when a total pressure loss coefficient relative to the exit dynamic pressure is given, entropy can only be estimated because the loss depends upon the as-yet unknown velocity distribution. Then an initial estimate of meridional velocities on all streamlines is required; this can be made by assuming the values determined at the previous station. Note that this is done on the first pass through all stations only. There are numerous possible combinations of data. Total temperature, total enthalpy, total temperature or enthalpy change from the previous station, total pressure or pressure ratio from the previous station are some of the possibilities. In conjunction with these, various efficiencies or loss coefficients may be prescribed. For test data analysis, and following a rotor, total temperature and total pressure will be the inputs. A significant amount of programming logic is required to navigate the choices. Equation (11.31) will be applied when relative flow angle is given or implied. A design calculation might specify flow angle rather than angular momentum at a stator discharge station, where test data will normally be total pressure and flow angle. (If total temperature is also measured, there is a choice to be made between convecting the temperatures from the leading edge station, or abandoning them and imposing the newly measured values. Some care would then be required with the overall thermodynamics of the calculation). Relative flow angle will be implied by any off-design performance calculation when blade geometry is the input data. This will require the estimation of losses and discharge flow angles by a cascade performance prediction scheme. Depending upon the scheme selected, the losses and/or flow angles may be dependant upon the as-yet unknown meridional velocities, leading only to estimates. Equation (11.29) or (11.31) is integrated, as was done in Step 6. If any of the data required for Eq. (11.29) or (11.31) could only be estimated, an iterative loop should be performed to obtain a meridional velocity distribution that is consistent with the performance modeling, although once a few overall passes have been performed any discrepancy should become very small.

(11) The continuity equation is applied as in Steps 7 and 8, with control passing back to Step 10 until the specified flow is achieved (or all permitted iterations have been performed). The stream function on each streamline will be required later.

(12) Control passes repeatedly back to Step 9 until the last station has been processed.

(13) The overall convergence of the calculation is checked, unless this point has been reached at the completion of the first pass. The following two criteria should be applied:
(a) The stream functions along each streamline should be constant, and
(b) The meridional velocities computed at each mesh point should not change from one pass to the next.
If convergence has been achieved, the desired output data may be generated (tolerances are discussed bellow). If convergence has not been achieved, and subject to a maximum permitted number of passes, control is passed to Step 14.

(14) The estimated streamline pattern for the entire machine may now be updated, the intent being to have the stream functions established at Station 1 maintained throughout. A simple interpolation of the streamline coordinates at each computing station using the Station 1 stream functions provides the new, raw streamline coordinates. In order to ensure a stable, convergent procedure a relaxation factor must be applied to the coordinate changes that the interpolation provides. This is discussed further below.

(15) All streamwise gradients are updated.

(16) Control passes back to Step 3, to start another pass.

(17) The relaxation factor required when relocating the streamlines is:

$$RF = \frac{1}{1 + \frac{A}{6}\left(\frac{h}{\Delta m}\right)^2} \tag{11.41}$$

where $h/\Delta m$ is the ratio of the station length to the meridional distance to the closest adjacent station, $A = (1 - M_m^2)$ if tangential velocity component is given, and $A = \cos^2\beta\,(1 - M_m^2)$ if relative flow angle is given. Occasionally the constant shown as 6 in Eq.(11.41) needs setting to 4. Typically this occurs when many stations are placed relatively close together, for example when multiple stations are placed within blade-rows. Although not supported by theory, it seems reasonable to limit the Mach numbers to maximum values of perhaps 0.7. These equations are based on Wilkinson [9].

Nested iterative calculations are involved in the solution procedure, and appropriate tolerances to judge convergence of each loop are needed. A master

tolerance should be defined by the input data, and this can be used for the outermost loop, that is, the streamline location and meridional velocity convergence check. For normal engineering purposes, a tolerance of 1 or 2 parts in 10^4 is adequate and easily obtained. If the results are to be used in a gradient-based optimization scheme, it may be necessary to reduce the master tolerance to 1 part in 10^7 or less.

Tolerances should be reduced by a factor of 5 or 10 for each successive nesting level. Several additional calculations can be integrated in the above procedure. Bleed flows can be modeled by arranging that at the first station, the desired bleed flows be contained within the outermost streamtubes. One or more streamlines are then removed at appropriate stations along the flow path. Overall pressure ratio can be specified for off-design calculations by estimating the corresponding flow, and then refining the estimate as the solution proceeds. Logic is required to handle the various failure situations that may occur, for example, choking of the machine when the estimated flow is too large. Loss models may be incorporated so that when a converged solution is achieved it includes losses consistent with the derived flow, both for design and off-design calculations. During design calculations, blade geometry may also be simultaneously generated.

A major shortcoming of the basic streamline curvature method lies in its use of the Euler equations: no transfer of momentum or heat occurs in the transverse direction. This is in contrast to both real flows and CFD solutions of the Navier-Stokes equations. The result is that realistic span-wise variations of losses cannot be specified through multi-stage machines because extreme profiles of properties typically develop. This can be largely overcome by superimposing a "mixing" calculation upon the basic streamline curvature calculation. While there is evidence that some of the transverse effects, such as radial wake movement in axial compressors, are not random (Adkins and Smith [10]), a simple turbulent mixing calculation, as suggested in Gallimore [11], seems to capture most important effects. With this addition to the flow-model, off-design calculations can be performed that include realistic span-wise variations of losses, and which result in realistic profiles of properties.

A momentum equation of somewhat different form to Eq.(11.29) and (11.31) is shown in Smith [12] . Here the gradient of meridional velocity in the meridional direction is eliminated through use of the continuity equation and streamline characteristics. This is aesthetically pleasing (at least) as it removes a streamwise gradient from those that must be updated from pass to pass. Further, for cases with few stations, such as when there are stations at blade-row edges only, intuitively it seems that the local streamwise velocity gradient might be better estimated from the streamline pattern than from velocities at points beyond a blade-row. In a case with many stations within all blade-rows, the differences should be very small. As presented, Smith's equation is less useful because it is framed in the radial rather than an arbitrary direction.

11.2.2 Examples

In this section some representative examples of the use of a streamline curvature program are shown. A design is pursued that aims to meet the targets defined by the NASA UEET project (as of 2003) for a four-stage aero-engine HP-compressor with an overall pressure ratio of 12:1.

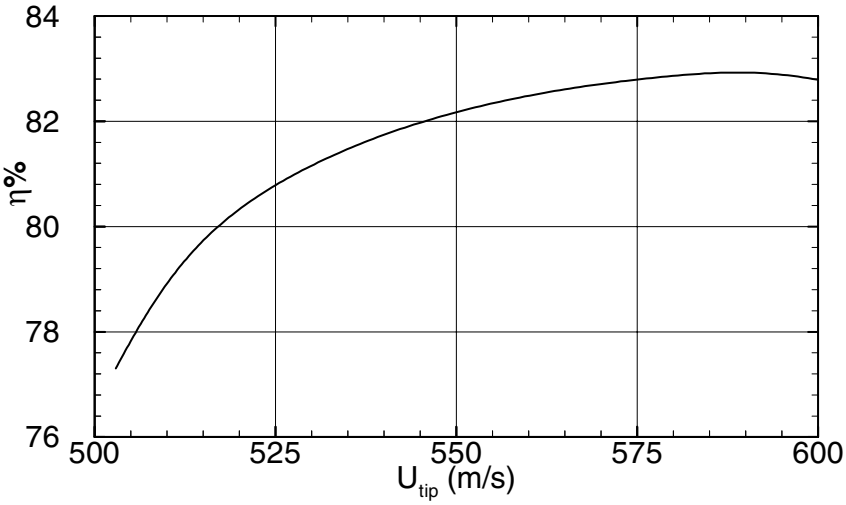

Fig. 11.3: Efficiency versus tip speed for NASA -UEET four stage compressor with pressure ratio 12:1

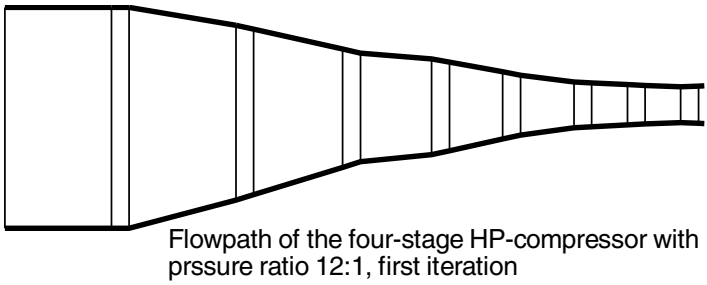

Fig. 11.4: Preliminary flow path of NASA -UEET four stage compressor.

The first calculations use the compressor preliminary design (CPD) procedure that is included in the program. In this mode of operation, streamline slope and curvature are assumed zero, and the blade forces acting in the station-wise direction are ignored. Radial stations are placed at each blade-row edge, so that a greatly simplified form of the momentum equation applies. These simplifications are made in order to stabilize and speed the solution. An optimizer package is used to derive the design of maximum efficiency that meets various constraints that the designer specifies. Figure 11.3 shows the resulting variation of design-point efficiency with first rotor tip speed. The optimum corrected tip of 589 m/sec results from the over-ambitious project goals. For the purposes of this rather academic exercise, a tip speed of 548 m/sec was selected as a possible compromise between mechanical and aerodynamic considerations. Figure 11.4 is the corresponding flow-path.

The next calculation made is a "first detail design". As for the CPD, total pressure is specified at rotor exits and tangential velocity component is specified at stator exits. Whereas for the CPD losses are estimated based solely on flow angles and Mach numbers, in the detail design blading, albeit generic, is derived by the design procedure. The flow model simplifications that were used for the CPD are

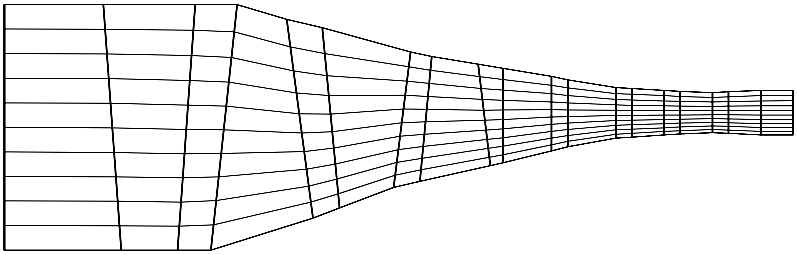

Fig. 11.5: Second iteration flow path of NASA UEET four-stage HP-compressor with pressure ration 12:1

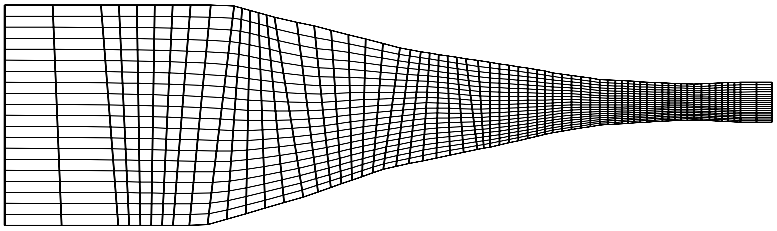

Fig. 11.6: Refined final flow path of NASA UEET four-stage HP-compressor with pressure ration 12:1

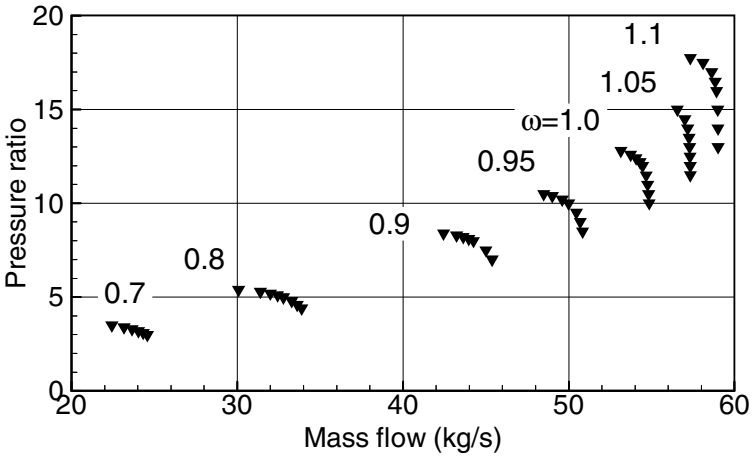

Fig. 11.7: Performance map of NASA UEET four-stage HP-compressor

removed. Figure 11.5 shows the computed streamline pattern. The first detail design assumed generic blading (DCA profiles), but with a first rotor tip Mach number approaching 1.5, a more sophisticated design is required.
This is accomplished by adding stations within the blade-rows, and then distributing the effects of the blade-rows amongst the station-to-station intervals. Figure 11.6

Fig. 11.8: Solid model of two adjacent blades.

shows the streamline pattern that is computed. Given the blading specification that the calculation created, an off-design calculation can now be performed; Figure 11.7 shows the resulting performance map. Figure 11.8 shows a solid-model of two adjacent blades, looking from downstream. The procedure described may be used to produce a final design, although nowadays it will generally be used to create a "first candidate" for further analysis using CFD.

11.3 Special Cases

The radial equilibrium calculation method derived in section 11.2 was applied to design compressor stages using numerical procedures. The method is also applicable to turbine stages. For few special cases analytical solutions can be found. For this purpose, simplifications are necessary to achieve analytical solutions.

11.3.1 Free Vortex Flow

The flow under consideration is assumed to fulfill the conditions: isentropic: $\nabla s = 0$, isoenergetic: $\nabla H = 0$, and constant meridional velocity, $dV_m = 0$. With these conditions and the assumption that the streamlines have no curvature, (cylindrical stream surfaces), Eq.(11.11) reduces for a bladeless channel, where $F_m = F_n = o$, and $(\phi - \gamma) = 0$, to:

$$d\left(rV_u\right) = 0,\ rV_u = \text{const.} \tag{11.45}$$

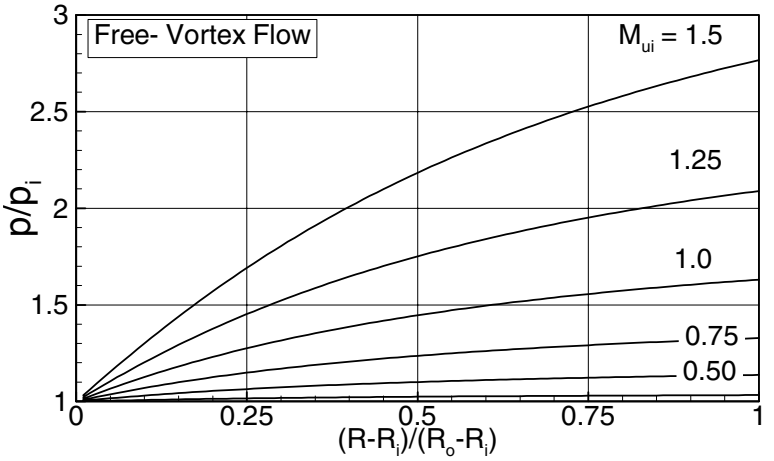

Fig. 11.9: Radial pressure distribution of a free-vortex flow with the hub circumferential Mach number M_u as parameter.

Eq.(11.45) is the radial equilibrium equation for a free vortex flow, called Beltrami free vortex flow. Figure11.9 shows the radial pressure distribution within an annular channel for different circumferential Mach number.

11.3.2 Forced vortex flow

This type of flow is assumed to satisfy the following conditions: isentropic, $\nabla s = 0$ isoenergetic, $\nabla H = 0$, and circumferential velocity is proportional to the radius: $V_u \propto r$ *or* $V_u = K$ r, where K is a constant.
With these conditions and the assumption that the streamlines have no curvature, (cylindrical stream surface), Eq.(11.11) reduces for a bladeless channel, where $F_m = F_n = o$, and $(\phi - \gamma) = 0$, to:

$$V_m \frac{dV_m}{dr} = - \frac{Krd(Kr^2)}{rdr} = -2K^2 \frac{rdr}{dr} \tag{11.46}$$

Integration of Eq.(11.46) gives:

$$V_m^2 = 2K^2\left(r_i^2 - r^2\right) + V_{mi}^2 \tag{11.47}$$

The constant K is:

$$K = \frac{V_u}{r} = \frac{V_{ui}}{r_i} \tag{11.48}$$

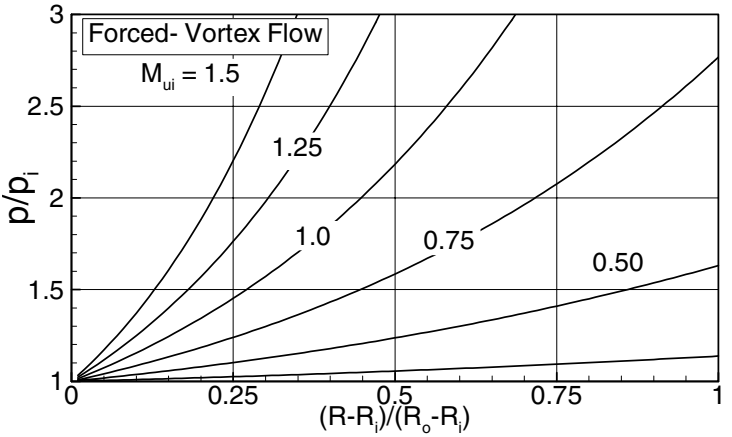

Fig. 11.10: Pressure distribution of a forced-vortex flow with the hub circumferential Mach number M_u as parameter.

Using the angle definition in Fig. 11.3, where β is replaced by α and $V_{ui} = V_{mi} tg\alpha_i$ and introducing Eq.(11.48) into (11.47) gives:

$$\left[\frac{V_m}{V_{mi}}\right]^2 = 1 - 2tg^2\alpha_i\left[\left(\frac{r}{r_i}\right)^2 - 1\right] \tag{11.49}$$

Figure 11.10 shows the radial distribution of meridional velocity ratio.

11.3.3 Flow with Constant Flow Angle

The flow under consideration is assumed to fulfill the conditions: isentropic, $\nabla s = 0$ isoenergetic, $\nabla H = 0$, and constant inlet flow angle, $d\alpha_1 = 0$. With these conditions and the assumption that the streamlines have no curvature, (cylindrical stream surface), Eq.(11.11) then reduces for a bladeless channel, where $F_m = F_n = o$, and $(\phi - \gamma) = 0$, to:

$$V_m \frac{dV_m}{dr} = -\frac{V_u}{r}\frac{d(rV_u)}{dr} \tag{11.50}$$

Since

$$V_u = V_m tg\alpha_1 \tag{11.51}$$

introducing Eq.(11.50) into (11.51) leads to:

$$\frac{dV_m}{V_m} = -\sin^2\alpha_1 \frac{dr}{r} \tag{11.52}$$

Integrating Eq.(11.52) gives:

$$\frac{V_m}{V_{mi}} = \left(\frac{r_i}{r}\right)^{\sin^2\alpha_1} \tag{11.53}$$

Figure 11.11 depicts the axial velocity ratio as a function of the radius ratio with α_1 as parameter.

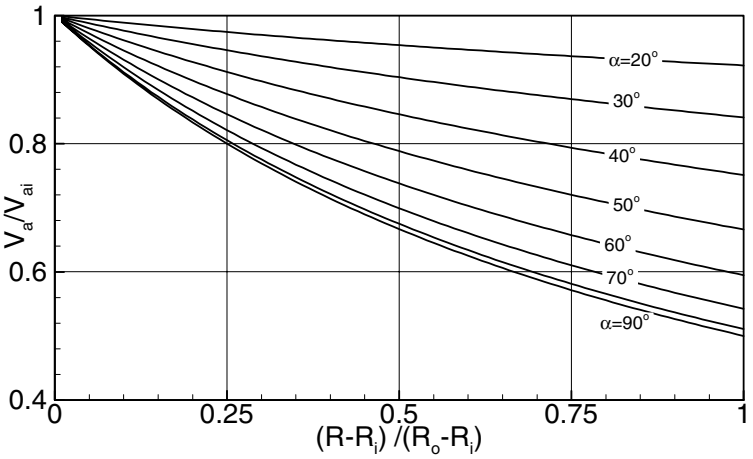

Fig. 11.11: Axial velocity ratio as a function of dimensionless blade height with the inlet angle as parameter.

References, Chapter 11

11.1 Wu, Chung-Hua, 1952, "A general Theory of Three-Dimensional Flow in Subsonic and Supersonic Turbomachines of Axial-, Radial, and mixed-Flow Types,"NACA technical Note 2604, Washington, D.C., January 1952.

11.2 Lakshminarayana, B., 1996, "Fluid Dynamics and Heat Transfer of Turbomachinery," John Wiley & Sons.

11.3 Vavra, M.H., 1960, "Aero-Thermodynamics and Flow in Turbomachines," John Wiley & Sons, Inc.

11.4 Novak, R. A., and Hearsey, R. M., " A Nearly Three Dimensional Intra blade Computing System for Turbomachinery, Part I & II," *Journal of Fluid Engineering*, Vol 99, pp. 154-166.

11.5 Wilkinson, D.H., 1972, "Calculation of Blade-to-Blade Flow in Turbomachine by Streamline Curvature," British ARC R&M 3704.

11.6 Wennerstrom, A. J., 1974, "On the Treatment of body Forces in the radial Equilibrium Equation of Turbomachinery," Traupel-Festschrift, Juris-Verlag, Zürich.

11.7 Hearsey, R. M., 2003, "Computer Program HT 0300 version 2.0," Hearsey technology, Bellevue, Washington

11.8 Horlock, J.H., 1971, "On Entropy Production in Adiabatic Flow in Turbomachines," *ASME Journal of Basic Engineering*, pp. 587-593.

11.9 Wilkinson, D.H., 1969, Stability, Convergence and Accuracy of 2-Dimensional Streamline Curvature Methods Using Quasi-Orthogonals, Proceedings of the Institution of Mechanical Engineers, Volume 184, 1979-1970.

11.10 Adkins, G. G., Smith L. H., 1982, "Spanwise Mixing in Axial-Flow Turbomachines," *ASME Journal of Engineering for Gas Turbines and Power*, Vol. 104, pp. 97-110.

11.11 Gallimore, S.J., 1986, "Spanwise mixing in Multistage Axial Flow Compressors: Part II – Throughflow Calculations Including Mixing," ASME Journal of Turbomachinery, Vol. 108, pp. 10-16.

11.12 Smith, L.H. Jr., 1966, "The Radial-Equilibrium Equation of Turbomachinery," *ASME Journal of Engineering for Power*, January, 1966, pp. 1-12.